Assessing the Ecological Role of Floods in the Elster–Luppe Floodplain Forest near Leipzig: Impacts on Tree Demography, Species Composition, Size Structure ,Biodiversity and Carbon Storage

Sabrina Akter
Chinmay Bhagwat
Benjamin Mensah
Joint International Master's in Sustainable Development
Inter- and Transdisciplinary Case Study
Dr Nadja Rüger
Dr. Julian Sagebiel
January 30, 2025

Table of Contents

Abstract

Forests on floodplains are constantly evolving communities addicted to periodic floods, particularly on floodplains. The alterations experienced by the floodplain forests are greatly affected by, and can impact, various ecosystem services. However, linking tree demography to functional biodiversity outcomes remains challenging, particularly across organism groups.

The aim of this study was to investigate the impacts of recurrent flooding on structural aspects and ecosystem functions in forests, and this was done in three different ways: first, by utilizing plot inventory data on trees in relation to flooded and non flooded plots to carry out tree demography, composition, diameter breast height, and rates of growth; second by applying them to conduct Perfect Plasticity Approximation (PPA) modelling to characterize structural elements in the forests, such as dominant crown size and structure; and third, by utilizing them with observations made on seasonal, monthly and daily intensities to conduct studies on surface runoff. Second, quantitative values for forest biodiversity value were generated by aggregating forest values, including data for tree basal area and species - specific beetle biodiversity relevance indices developed by an independent beetle survey working group. Third Carbon values were estimated by utilizing DBH based relationships, including a method for quantifying species based forest carbon values as an estimate of above ground forest carbon by species.

The model results indicated that differences in forest structures due to flooding were highlighted in all three approaches. Parameterization of PPA indicated particularly dominant forms in relation to forest structure caused by a few tree species. Value of biodiversity was particularly promoted by structurally dominant tree forms with high biodiversity value in relation to beetle diversity, particularly oak due to its importance in terms of volume and relevance to beetles. Value to carbon stock also indicated dominance effects, whereby larger trees dominated in terms of total volume of carbon. Growth rate did not provide any value in relation to biodiversity value and carbon stock.

The study shows in general that flooding influences forest ecosystem functioning mainly by means of its effects on forest structure. Structurally dominant tree species are the most important factor in determining biodiversity value and carbon storage in floodplain forests, underlining the need to combine forest demography with structural modelling and functional indicators when assessing the impacts of flooding.

1. Introduction

1.1 Background

Floodplain forests are among the most dynamic and productive terrestrial ecosystems, shaped by periodic inundation, sediment deposition, and strong hydrological gradients. These ecosystems are characterized by frequent disturbance regimes that regulate species composition, stand structure, and nutrient availability. Floodplain forests provide extraordinarily diverse habitats for many plants and animals species and therefore play a crucial role in preserving biodiversity (Elles et al.,2021). As a result, floodplain forests provide essential ecosystem services, including biodiversity conservation, carbon sequestration, flood mitigation, water purification, and nutrient cycling (Naiman et al., 2005).

Despite their ecological importance, floodplain forests across Europe have been extensively altered by river regulation, channelization, embankment construction, and flood control measures. These interventions have reduced flood frequency and duration, disrupted natural sediment dynamics, and weakened hydrological connectivity between rivers and their floodplains. Consequently, many floodplain forests have experienced shifts in species composition, reduced structural heterogeneity, and declines in ecosystem functioning (Tockner et al., 2010). Understanding how restored or recurrent flooding influences forest dynamics is therefore critical for effective floodplain restoration and long-term ecosystem management.

1.2 Knowledge gap

Most floodplain forest research has historically focused on vegetation composition, habitat heterogeneity, and short-term structural indicators such as basal area or canopy openness (Ward et al., 2002). While these studies have been critical for understanding ecosystem patterns, they often overlook the demographic processes growth, mortality, and recruitment that ultimately drive long-term forest development. Without explicitly quantifying these demographic rates, it is difficult to predict future forest trajectories under altered hydrological regimes or restoration scenarios.

The Elster–Luppe floodplain forest near Leipzig, Germany, provides a unique opportunity to address this gap. Through the *Lebendige Luppe* restoration project, near-natural flooding has been partially restored by reconnecting former river channels and allowing controlled inundation events. The availability of repeated forest inventories from both flooded and non-flooded plots allows for a direct comparison of demographic responses under contrasting hydrological

conditions. This study therefore moves beyond descriptive indicators and focuses on species-specific demographic rates as mechanistic drivers of forest dynamics.

1.3 Research Question

The central research question guiding this study is:

To what extent do recurrent flooding regimes modify forest tree demography, species composition, and size structure, and how do these structural and compositional changes influence biodiversity value and carbon storage in floodplain forests?

This question explicitly links hydrological disturbance to demographic mechanisms and ecosystem-level outcomes, integrating population processes with broader conservation and management objectives.

1.4 Research Objectives

To address this question, the study pursues the following objectives:

1. To quantify species-specific growth, mortality, and recruitment rates and evaluate the impacts of flooding by analysing inventory data from three flooded and two non-flooded forest plots in the Lebendige Luppe floodplain restoration project.
2. To project tree species composition and forest size structure in flooded and non-flooded plots for the period 2020–2070 using the Perfect Plasticity Approximation (PPA) model.
3. To assess biodiversity value (Project 1) and carbon storage (Project 2) across alternative flooding and non-flooding scenarios.

2. Methodology

2.1 Study Area

The study area is located in the Elster–Luppe Aue, a floodplain of alluvial forests and meadows northwest of Leipzig. The floodplain is shaped by the Weiße Elster and Luppe rivers; however, the development of the Neue Luppe canal has disconnected the landscape from natural water dynamics. This regulation lowered groundwater levels and degraded typical floodplain conditions (Landesamt für Umweltschutz Sachsen-Anhalt, 2000)

The *Lebendige Luppe* project is working to reverse this by reactivating former river channels. By connecting the forest to the Weiße Elster, the project intends to restore seasonal floods and enhance ecosystem services including biodiversity and flood management (Lebendige Luppe, n.d.; (Helmholtz Centre for Environmental Research (UFZ), 2024)).

2.2 Plot Design and Inventory Data

This study analyzed five 0.25-ha plots from the Lebendige Luppe network: three flooded sites (81–83), which have been regularly inundated since 1993 (Helmholtz Centre for Environmental Research [UFZ], 2024), and two non-flooded reference sites (84, 86).

For plots 81, 82, 84, and 86, the project advisor provided inventory data for 2020 and 2024. From this dataset, specific variables including tree codes, tree IDs, diameter at breast height (DBH), canopy layer, and tree status were extracted. For plot 83, although 2020 data were available, the 2025 inventory was collected with the UFZ team as part of coursework.

Throughout the study seven focal tree species were analyzed and identified by the following codes: BAH (*Acer pseudoplatanus*), GES (*Fraxinus excelsior*), HBU (*Carpinus betulus*), SAH (*Acer platanoides*), SEI (*Quercus robur*), UL (*Ulmus* spp.), and WLI (*Tilia* spp.).

2.3 Field Data Collection And Remeasurement

Inventory data for plot 83 were collected in 2025 together with the UFZ team. During this fieldwork, we were responsible for collecting recruitment data and the UFZ team collected the remaining inventory variables.Recruiting trees were defined as individuals of tree species above a minimum size threshold (DBH ≥ 5 cm at 1.3 m height) (Engelmann et al., 2022). For each recruiting tree, diameter at breast height (DBH) was measured with a DBH tape placed at 1.3 m

above ground. Tree height was then determined using an ultrasonic hypsometer in combination with a clinometer and measuring tape to obtain the required distance and angle measurements. Finally, the spatial position of each recruiting tree within the plot was recorded relative to a known reference tree, using compass bearings and tape-measured distances to reconstruct the location of each individual in a local plot coordinate system.

2.4 Estimation Of Demographic Rates

Demographic rates were estimated from repeated tree inventories (2020–2024/2025) in three flooded plots and two non-flooded plots, calculated separately by plot type. Tree records were first processed and standardised to obtain consistent species codes, to classify plots by hydrological type (flooded vs. non-flooded), and to assign trees to canopy layers (coded as 1 = overstory and 2 = understory).In total, the analysed dataset comprised 496 tree records in the flooded plots and 438 in the non-flooded plots across the two censuses. The specific methods for calculating growth, mortality, and recruitment are discussed in the following sub-sections .

2.4.1 Growth

Annual DBH growth was calculated only for surviving trees with valid DBH measurements at both censuses and a known census interval. For each individual tree

$$\text{Annual Growth(cm/yr)} = \frac{DBH_{2024/25} - DBH_{first\ inventory}}{\Delta t}$$

where $DBH_{2024/25}$ and $DBH_{first\ inventory}$ are diameters at breast height (cm) at the second and first census, and Δt is the census interval in years (Boyce et al., 2024b).

Dividing the DBH increment by the census interval (Δt) standardised growth rates to cm year^{-1}, allowing direct comparison across plot types. To reduce the influence of measurement errors and extreme outliers, only growth values within the range [−1,1] cm year^{-1} were retained for analysis, and observations outside this range were excluded from the calculation of mean growth (Figure A1).

2.4.2 Mortality

Dead trees were identified using two specific criteria: (1) trees with a positive DBH in 2020 but recorded as DBH = 0 in the latest census, and (2) assigned mortality status codes (“2 = zu THS” or “4 = zu THL”). Trees meeting either condition were classified as dead for mortality calculations.

For each species and canopy layer within a plot type, the raw interval mortality proportion (μ_{raw}) was calculated as:

$$\mu_{raw} = \frac{N_{dead}}{N_{total}}$$

Here, N_{dead} shows the number of trees classified as dead between censuses and N_{total} the number of individuals alive in 2020 with a positive DBH(Roman & Scatena, 2011). This proportion was then converted to an μ_{annual} annual mortality probability calculated as :

$$\mu_{annual} = 1-(1-\mu_{raw})^{1/\Delta t}$$

where Δt is the census interval in years (Roman & Scatena, 2011). This conversion standardizes annual probabilities across different census periods while assuming a constant mortality risk. The final species- and canopy-specific rates were calculated by averaging these probabilities for each plot type.

2.4.3 Recruitment

Species-level recruitment was calculated for flooded and non-flooded stands.Recruits were defined as individuals absent in 2020 that subsequently reached the measurement threshold in the latest census or were coded '5 – BAUM Neu' in the dataset. Final estimates were derived using the following equation:

$$\text{Recruitment rate} = \frac{Number\ of\ recruits}{Plot\ area \times Census\ Interval}$$

yielding recruitment in trees ha^{-1} year^{-1} for (i) flooded plots 81–82 (0.50 ha), (ii) flooded plots 83 (0.25 ha) and (iii) non-flooded plots 84–86 (0.50 ha).For the flooded stands, these estimates were weighted by plot area to correct for size differences, producing a single standardized mean.

2.5 PPA Model Setup And Simulations For 2020–2070

2.5.1 Forest demographic model framework description and implementation

The Perfect Plasticity Approximation (PPA) framework, which models the forest as cohorts defined by species, diameter, and canopy layer, was used in demographic simulations (Elles et al., 2024). In order to simulate asymmetric light competition, the model dynamically reassigns

cohorts to vertical layers depending on crown area, allowing top canopies to occupy available space first. (Elles et al., 2024).

This study adjusted the temporal resolution to a 5-year time interval across a 50-year projection, starting with 2020 inventory data. Cohort density and size were updated at each interval using species- and layer-specific growth, mortality, and recruitment rates, predicting future stand composition under both flooded and non-flooded conditions.

2.5.2 Model Parameterization

Demographic parameters were estimated from the inventory, which is described in Section 2.4.However growth rates for Fraxinus excelsior in canopy layer 2 and mortality estimates for several species in both plot types could not be derived from the available dataset. Therefore missing values were substituted with demographic rates from the intermediate groundwater-distance class reported by Boyce et al. (2025).Crown allometry parameters (A–D) were also adopted from this source to define the DBH–crown area relationship. The final parameter set is detailed in Appendix A (Tables A.2, A.3).

2.5.3 Initial conditions and scenarios

The initial state of the forest was defined using 2020 inventory data. Trees from the seven focal species were first aggregated into two plot types: flooded (0.75 ha) and non-flooded (0.50 ha). Cohorts were then structured by 1-cm DBH bins (5–152 cm), stem density (trees ha^{-1}), canopy layer (overstory vs. understory), and species identity. Stem densities were calculated by dividing total counts per bin by the respective plot area, while canopy layers were assigned based on field data (defaulting missing values to overstory)

2.5.4 Simulation Output

Simulations generated cohort-level data and stand summaries at 5-year intervals. These results were analyzed to observe trends in basal area and stem density for each species over a 50-year period. Cohorts were grouped into specific DBH classes (ranging from 0–10 cm to >80 cm) in order to evaluate structural shifts. This allowed for a direct comparison of size distributions between the first and last simulation years.

2.6 Quantification Of Biodiversity And Carbon Storage

2.6.1 Tree Demography and Forest structure

Tree demography and forest structure were characterized using tree composition, abundance, diameter distribution, and tree growth rates. Tree diameter at bread height (DBH) was used as the major tree size and structural dominance attribute because of its strong relationship with biomass production and habitat availability in forest ecosystems (Pretzsch, 2009).
Growth rates were obtained through repeated measures of tree DBH and used to investigate differences in tree performance across tree species. Species were aggregated into groups using standardized short species codes. These tree demography variables formed the basis for further analysis of forest structure, biodiversity value, and carbon storage.

2.6.2 Biodiversity Value Estimation

Forest biodiversity value was quantified by integrating tree structural dominance with beetle habitat relevance. Structural dominance was assessed using basal area, calculated for each tree from DBH as:

$$\text{Basal area} = \pi \times \left(\frac{\text{DBH}}{2}\right)^2$$

With DBH expressed in meters. The basal area was summed by a tree species group and used as a proxy for habitat quantity and structural importance within the forest stand.

Biodiversity value was calculated by weighting the basal area of each tree species group by its corresponding beetle diversity relevance index. For each species group i, the contribution to forest biodiversity value was calculated as:

$$\text{Contribution}_i = \text{Basal area}_i \times \text{Beetle relevance}_i$$

The forest level biodiversity value index was calculated by adding all species group values. This method combines habitat amount (tree structure) and habitat quality (beetle relevance) in a single index and adheres to a conceptual model that structurally dominant tree species with high

habitat relevance support forest biodiversity disproportionately (Southwood, 1961; Seibold et al., 2015)

2.6.3 Carbon Storage Estimation

For the estimation of the above ground carbon storage, the DBH-based allometric relationships were used. In this study, the diameter of the trees was used as a measure of the above ground biomass using the standard power law relationship between DBH and biomass, which is commonly used in forest ecology and carbon accounting (Chave et al., 2014).

Assumptions about biomass composition were made to convert biomass estimates to carbon pools, assuming 50% of biomass is carbon. This assumption is consistent with other forest carbon studies (Pan et al., 2011). Individual tree carbon pools were calculated and then grouped by tree species to quantify the relative contributions of different species to total carbon pools. Carbon storage calculations were conducted independently from biodiversity analyses to ensure a clear separation between ecosystem functions.

2.7 Statistical Analysis And Software

Data preparation was carried out in Microsoft Excel. All further data processing and statistical analyses, including calculation of demographic rates and implementation of the PPA model were performed in R (version 4.5.1)

3. Results

3.1 Demographic Dynamics

3.1.1 Flooded Data

Demographic rates for the flooded scenario were calculated from repeated inventory data collected in three (3) permanently flooded plots within the Elster–Luppe floodplain, representing long-term inundation conditions. These data capture species- and canopy-specific responses of growth, mortality, and recruitment to sustained flooding.

Table 1

Flooded Demographic Rates

Sp	G1	G2	MU1	MU2	Re./h
BAH	0.2114	0.1693	0.0382	0.0332	0.6667
GES	0.1981	0	0.0653	0	0.2667
HBU	0.3286	0.3422	0	0	2.6667
SAH	0.4658	0.3688	0	0	3
SEI	0.3306	0.1643	0.0031	0.0271	0
UL	0.5179	0.4673	0.0682	0.0199	5.4667
WLI	0.523	0.4679	0	0.002	10.6

3.1.2 Non-Flooded Data

Demographic rates for the non-flooded scenario were derived from repeated inventory data collected in two non-flooded reference plots within the Elster–Luppe floodplain, representing conditions without regular inundation. These data capture species- and canopy-specific patterns of growth, mortality, and recruitment in the absence of flooding.

Table 2

Non-Flooded Demographic Rates

Sp	G1	G2	MU1	MU2	Re./h
BAH	0.4364	0.5473	0.0312	0	72.5
GES	0.0559	0	0.0515	0	0
HBU	0.375	0.3833	0	0	0.5
SAH	0.5938	0.5114	0	0	11
SEI	0.2404	0.3	0	0	0
UL	0.3375	0.3422	0.029	0	1.5
WLI	0.4679	0.4739	0	0	2

3.1.3 Growth Rates

Growth rates varied strongly among species, flooding regimes, and canopy layers. Across both flooded and non-flooded plots, overstory trees consistently exhibited higher growth rates than understory individuals, reflecting greater light availability.

Figure 1

Graphical representation of growth rate results

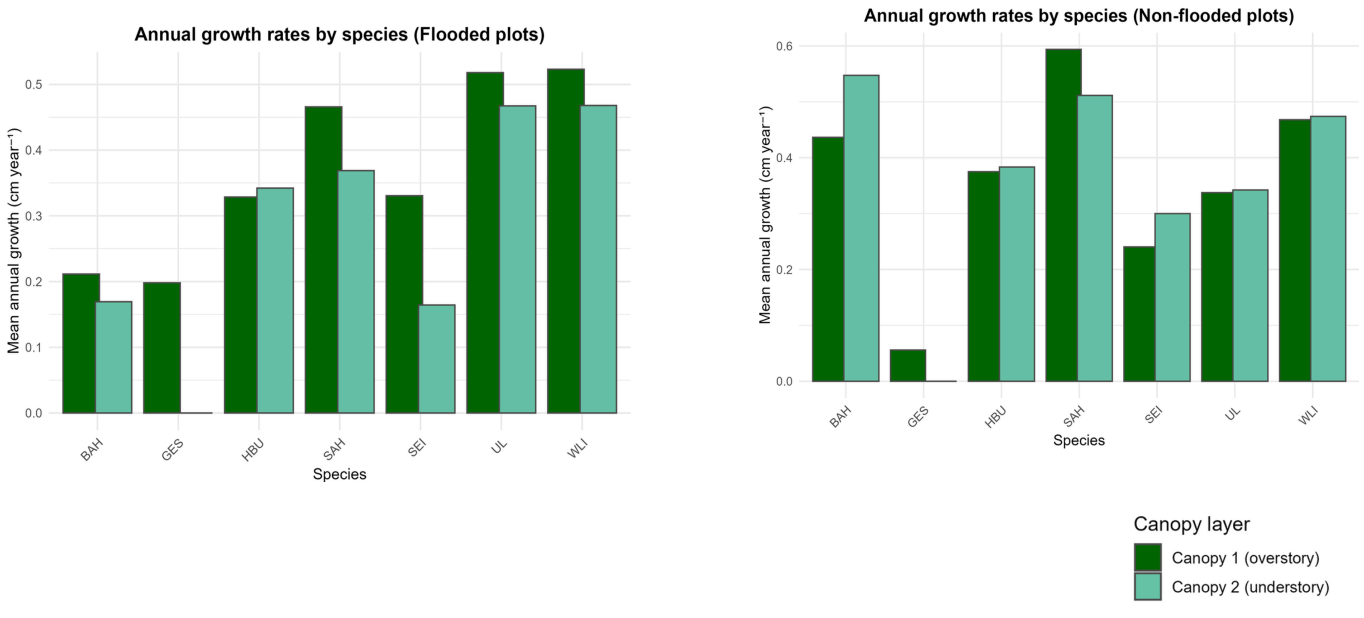

In flooded plots, flood-tolerant and shade-tolerant species such as lime (*Tilia cordata*), hornbeam (*Carpinus betulus*), and elm (*Ulmus* spp.) maintained moderate to high growth rates in both canopy layers, indicating strong physiological adaptation to waterlogged soils. In contrast, sycamore maple (*Acer pseudoplatanus*) and ash (*Fraxinus excelsior*) showed reduced growth under flooded conditions, particularly in the understory, likely due to oxygen limitation, flood stress, and heightened competition. In non-flooded plots, maple species exhibited higher growth rates, especially in the overstory, reflecting favorable soil aeration and competitive light capture. Oak (*Quercus robur*) displayed consistently low but stable growth across both flooding regimes and canopy layers, suggesting persistence rather than competitive growth dominance. Overall, the observed growth dynamics indicate that flooding selectively favors flood- and shade-tolerant species while constraining growth of light-demanding and flood-sensitive species.

3.1.4 Mortality Rates

Observed mortality rates were low across all species, flooding regimes, and canopy layers. Overstory trees generally exhibited lower mortality than understory individuals, consistent with greater structural stability and carbon reserves in larger trees. In both flooded and non-flooded plots, flood- and shade-tolerant species such as lime (*Tilia cordata*), hornbeam (*Carpinus betulus*), and oak (*Quercus robur*) showed little to no detectable mortality. Part of this low observed mortality is attributable to the limited sample size and short census interval, which reduce the probability of capturing mortality events, particularly for long-lived tree species. Ash (*Fraxinus excelsior*) showed relatively higher mortality compared to other species, especially in the overstory, likely reflecting disease-related decline rather than direct flooding effects. Overall, the results suggest that while flooding does not appear to cause immediate increases in tree mortality, conclusions regarding mortality patterns should be interpreted cautiously due to small sampling size.

Figure 2

Mortality rates in flooded and non-flooded scenario

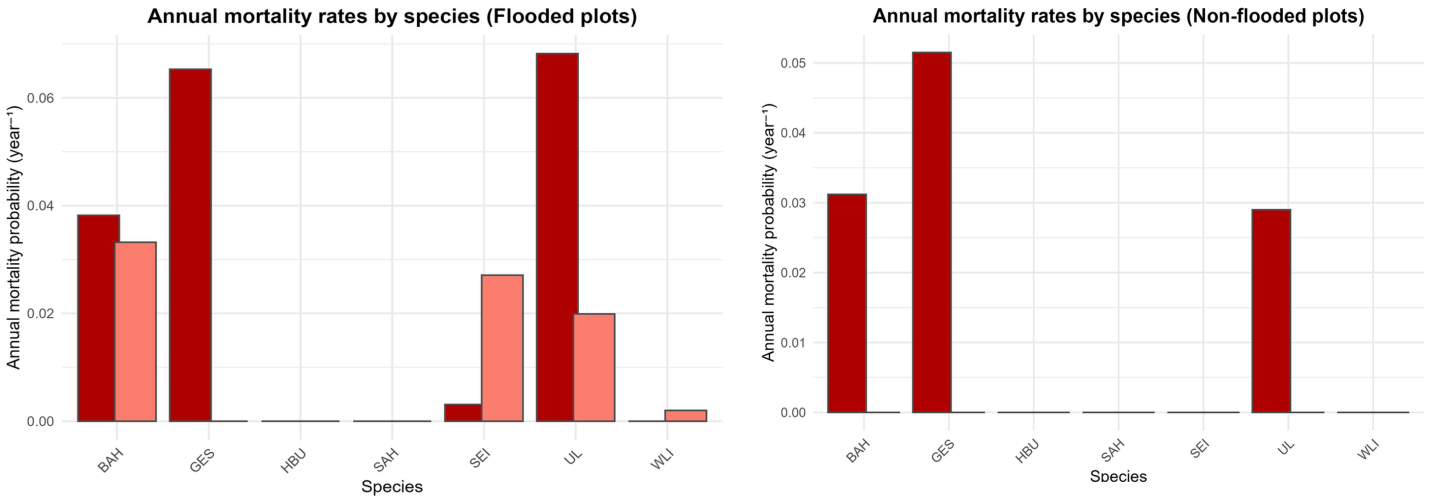

3.1.5 Recruitment Rates

Recruitment rates varied markedly among species and flooding regimes, reflecting strong differences in regeneration strategies and flood tolerance. In flooded plots, recruitment was dominated by flood- and shade-tolerant species, particularly lime (*Tilia cordata*) and elm (*Ulmus* spp.), indicating successful establishment under periodic inundation and low-light conditions. In contrast, sycamore maple (*Acer pseudoplatanus*) exhibited reduced recruitment in flooded plots despite high seed production, suggesting sensitivity of early life stages to prolonged soil saturation. Oak (*Quercus robur*) showed consistently low recruitment across both flooded and non-flooded plots, reflecting its reliance on episodic high-light conditions and vulnerability of seedlings to flooding-induced root destabilization. In non-flooded plots, maple species displayed higher recruitment rates, consistent with favourable soil aeration, high shade tolerance during early development, and effective seed dispersal. Overall, the recruitment patterns indicate that flooding acts as a strong ecological filter during early life stages, promoting flood-tolerant species while constraining regeneration of flood-sensitive and light-demanding species, thereby shaping future forest composition.

Figure 3

Recruitment rates in flooded and non-flooded scenario

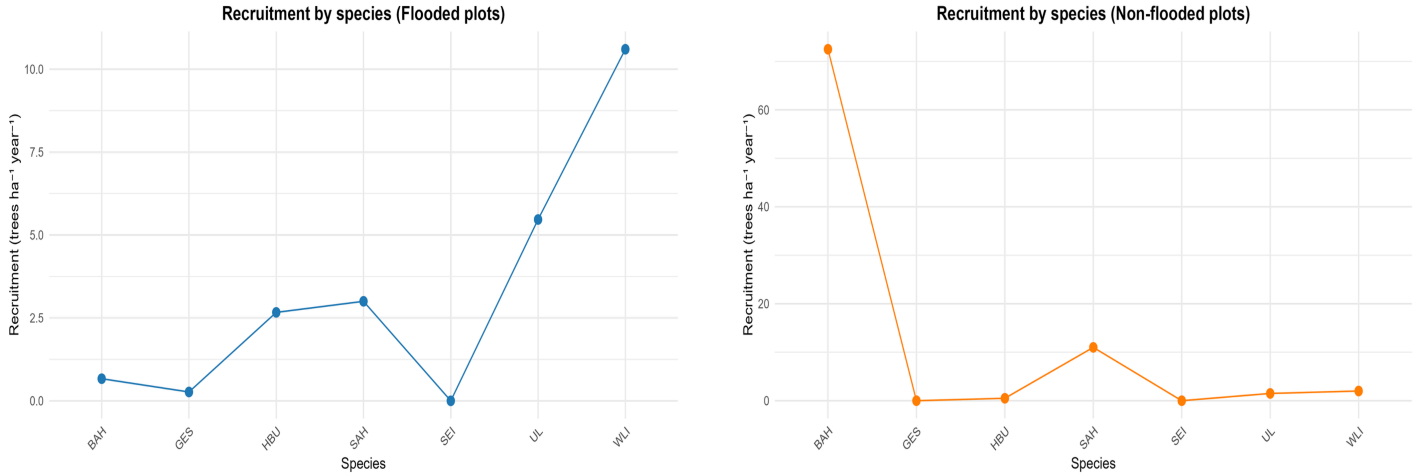

3.1.6 Comparison with Reference

3.1.6.1 Growth Rate

Growth patterns across flooded and non-flooded plots closely matched those reported by Elles

(2025), despite differences in sample size and spatial extent. Flood- and shade-tolerant species such as lime (*Tilia cordata*), hornbeam (*Carpinus betulus*), and elm (*Ulmus* spp.) showed moderate to high growth in flooded plots across both canopy layers, consistent with the reference study. Maple species exhibited higher overstory growth in non-flooded plots and in Elles (2025), while ash (*Fraxinus excelsior*) showed reduced growth across all datasets, likely reflecting disease impacts. Oak (*Quercus robur*) displayed low but stable growth in flooded, non-flooded, and reference plots.

Figure 4
Recruitment rate

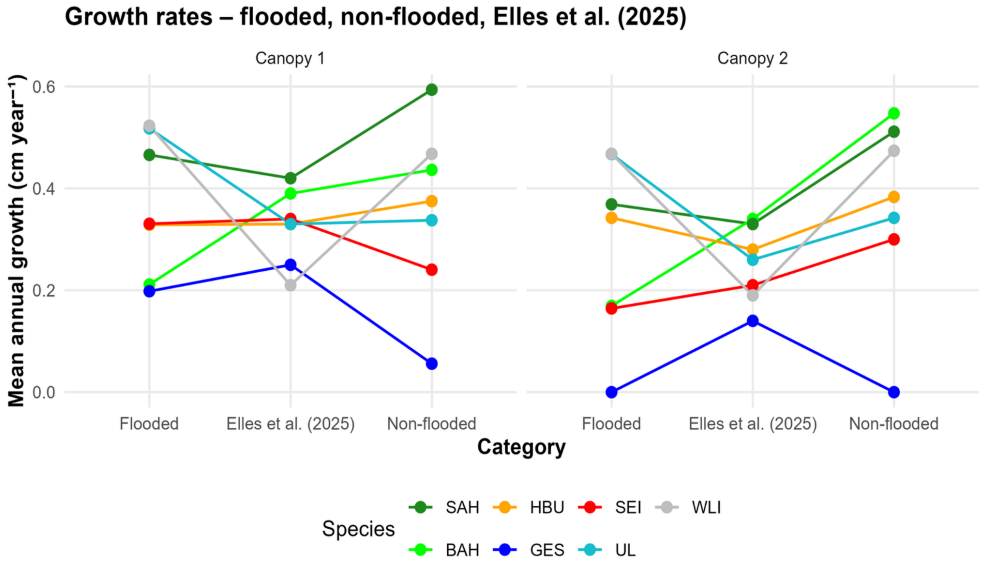

3.1.6.2 Mortality Rate

Mortality rates were low across species and canopy layers in both this study and Elles (2025). Lime, hornbeam, and oak exhibited negligible mortality across flooded, non-flooded, and reference plots, indicating high tolerance to hydrological and competitive stress. Ash showed comparatively higher mortality in all datasets, particularly in the overstory, consistent with regional ash decline. Differences in absolute mortality values are likely due to the larger plot network and longer census period in Elles (2025).

Figure 5

Mortality rate

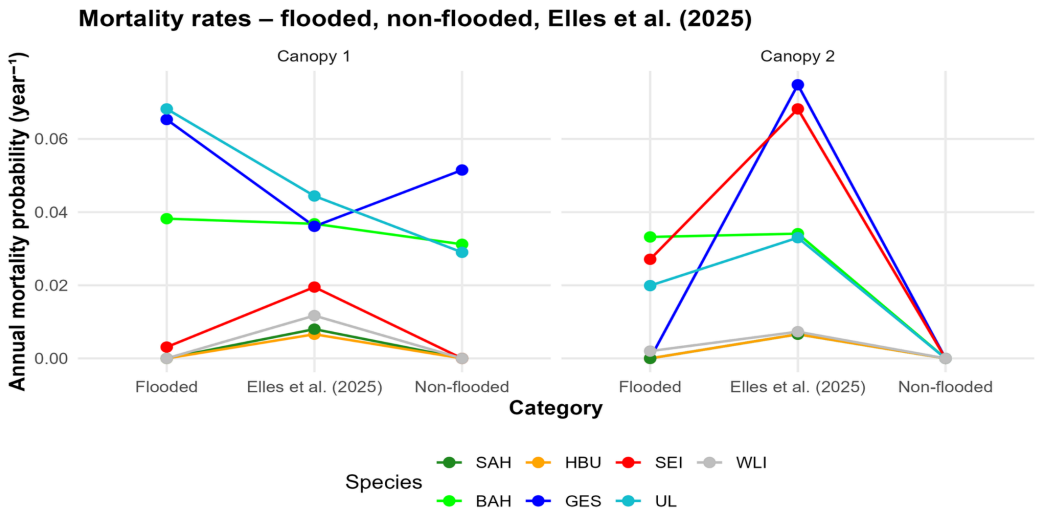

3.1.6.3 Recruitment Rate

Recruitment patterns were highly consistent across studies. In flooded plots and in Elles (2025), recruitment was dominated by flood-tolerant species such as lime and elm. Maple species recruited more strongly in non-flooded plots and in the reference data but showed reduced recruitment under flooded conditions. Oak recruitment remained low across all datasets and canopy layers, confirming strong regeneration limitations in floodplain forests.

Figure 6

Recruitment rate

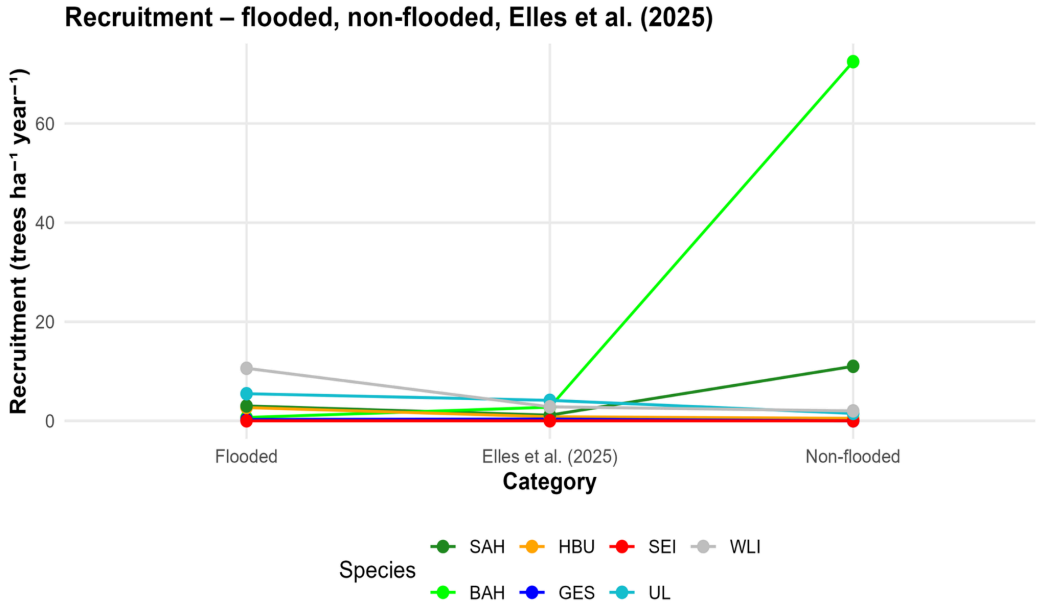

3.2 Perfect Plasticity Approximation (PPA) Model Projections: Species Composition and Size Structure

3.2.1 Species composition over time

The PPA simulations show a significant transformation of species-level basal area during the 50-year timeframe in the flooded plot. (Table 3,Figure 7).

Table 3

Comparison of species basal area and percentage change between year 0 and year 50 in flooded plots

sp	ba_t0	ba_t50	%change
BAH	0.54	0.17	-67.87
GES	4.3	0.2	-95.45
HBU	6.77	12.68	87.3
SAH	0.27	2.32	762.14
SEI	15.37	18.72	21.78
UL	0.74	3.48	371.87
WLI	1.07	13.35	1148.96

Figure 7

Simulated Changes in Species-Level Basal Area Ove a 50-Year Timeframe in Flooded plots

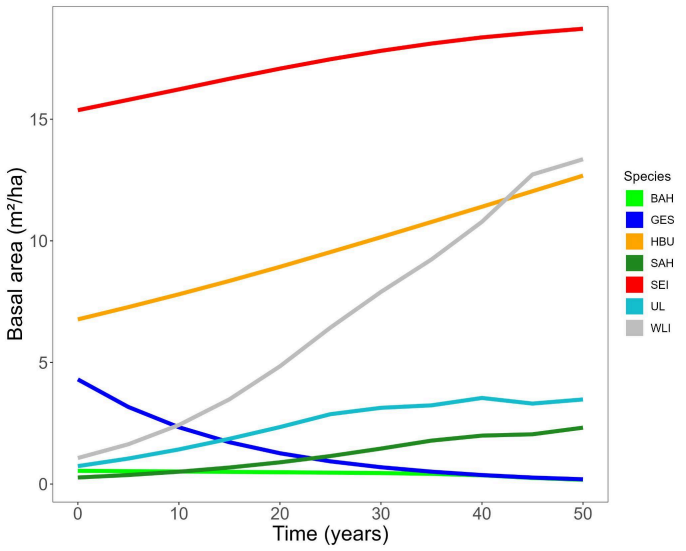

Note. Abbreviations: sp = species; ba_t0 = basal area at year 0; ba_t50 = basal area at year 50; %change = percentage change. Species codes: BAH = *Acer pseudoplatanus*; GES = *Fraxinus excelsior*; HBU = *Carpinus betulus*; SAH = *Acer platanoides*; SEI = *Quercus robur*; UL = *Ulmus* spp.; WLI = *Tilia* spp.

Fraxinus excelsior (GES) and *Acer pseudoplatanus* (BAH) lost significant basal area over the 50 years, dropping by 95% and 68% respectively. In comparison, Quercus robur (SEI) remained stable. Other species, including Tilia spp. (WLI), Ulmus spp. (UL), Carpinus betulus (HBU), and Acer platanoides (SAH), all increased in basal area. This growth was strongest for WLI and SAH. Specifically, WLI grew from 1.07 to 13.35 m²/ha, while SAH went from 0.27 to 2.32 m²/ha.The rapid expansion of WLI is likely linked to the low mortality rates of canopy-layer-2

Tilia trees in the input data, which influenced the PPA model. Overall, the stand shifted from being dominated by SEI, HBU, and GES to a mix of WLI, HBU, UL, and SEI.

The model projects a different pattern of species composition in non-flooded conditions compared to flooded conditions (Table 4, Figure 8).

Table 4

Comparison of Species Basal Area and Percentage Change Between Year 0 and Year 50 in non-flooded plots

sp	ba_t0	ba_t50	%change
BAH	4.3	19.08	343.82
GES	11.88	0.92	-92.25
HBU	0.51	1.15	127.4
SAH	0.45	7.76	1632.68
SEI	13.59	6.65	-51.02
UL	0.52	0.42	-20.56
WLI	1.96	4.63	135.81

Figure 8

Simulated basal area (m²/ha) of tree species at year 0 and after 50 years in non- flooded plots

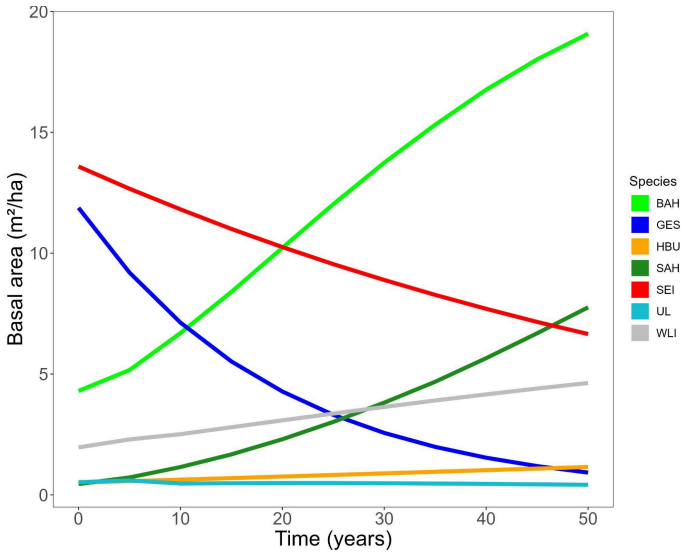

Note. Species codes and abbreviations are identical to those defined in Table 3

At year 0, the stand basal area is dominated by *Quercus robur* (SEI), *Fraxinus excelsior* (GES), *Acer pseudoplatanus* (BAH), and *Tilia* spp. (WLI), while *Acer platanoides* (SAH), *Ulmus* spp. (UL), and *Carpinus betulus* (HBU) play a minor role. Over the 50-year simulation, the basal area of BAH and SAH increases steeply, by approximately 344% and 1,633% respectively, making both species major components of the future forest stand. HBU and WLI also show moderate gains of roughly 127% and 136%. In contrast, GES and SEI decline strongly, with reductions of 92% and 51% respectively. Overall, the simulations indicate a shift from an SEI-GES-BAH-WLI dominated stand at year 0 towards a composition increasingly dominated by BAH, SAH, SEI, and WLI under non-flooded conditions.

3.2.2. Stand Size Structure by DBH Class

3.2.2.1 Basal Area Distribution Across DBH Classes

The PPA simulations show clear differences in size structure between flooded and non-flooded plots (Figure 9).

Figure 9

Simulated basal area by DBH class at year 0 and after 50 years for flooded and non-flooded plots

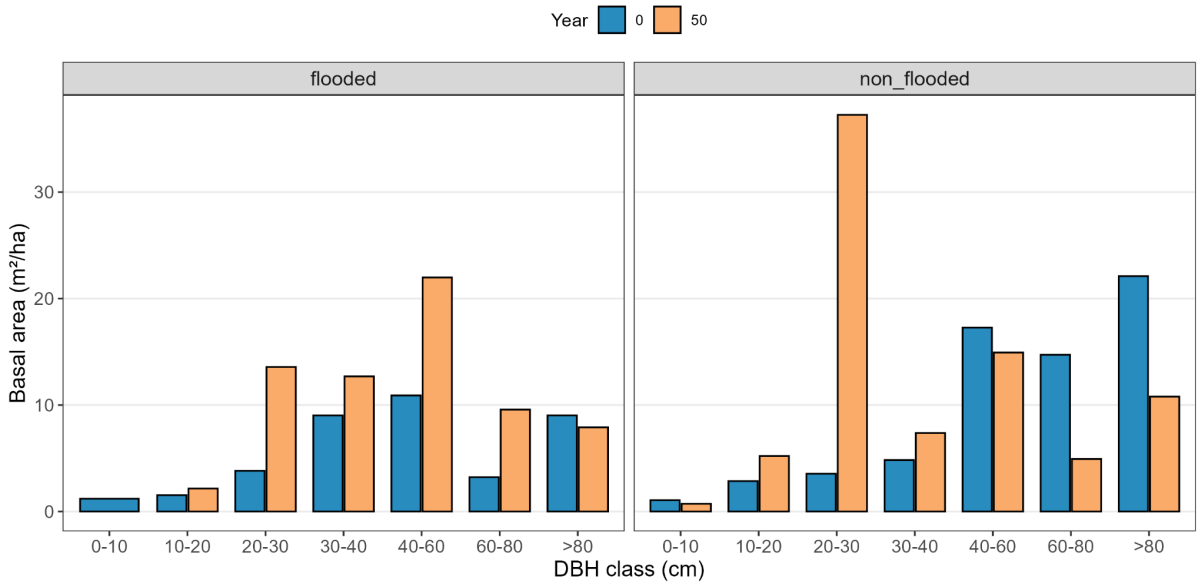

Note. DBH = Diameter at Breast Height (1.3 m). Basal area is summed per diameter class (m²/ha). Blue bars = Year 0; Orange bars = Year 50.

In flooded plots, basal area at year 0 is concentrated in intermediate and large trees (30–60 cm and >80 cm DBH). After 50 years, basal area increases in almost all size classes, with the strongest increase in the 40–60 cm class. In non-flooded plots, the basal area at year 0 is dominated by large trees in the 40–60 cm and >80 cm classes. By year 50, basal area shifts strongly toward the 20–30 cm class, while the largest classes lose basal area.

3.2.2.2 Tree Density Distribution Across DBH Classes

Stem density patterns also change strongly across size classes (Figure 10).

Figure 10

Simulated stem density (trees/ha) by DBH class at year 0 and after 50 years for flooded and non-flooded plots.

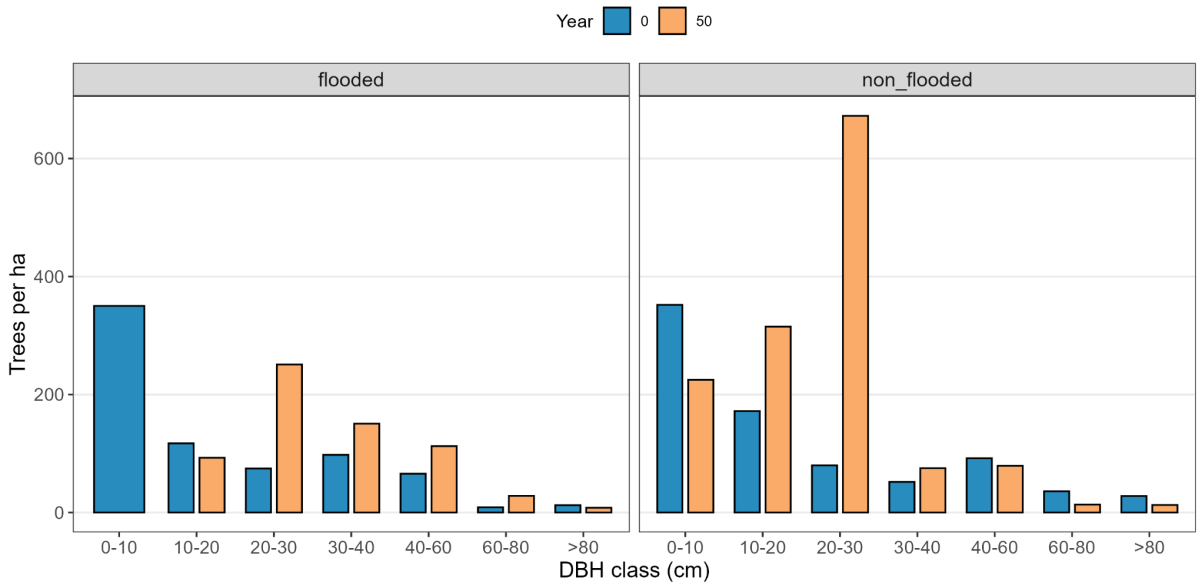

Note. DBH = Diameter at Breast Height (1.3 m). Values represent stem density (number of trees per hectare). Blue bars = Year 0; Orange bars = Year 50.

In flooded plots at year 0, there is a very high density of small stems (0–10 cm DBH), with densities declining toward larger classes. After 50 years, densities in the 20–60 cm classes increase, while very few stems remain above 60 cm. In non-flooded plots, initial densities are concentrated in the 0–20 cm classes, with low densities in larger trees. By year 50, a pronounced peak develops in the 20–30 cm class, whereas densities in the largest classes stay low.

3.2.3 Basal area–density relationship

The simulations show contrasting 50-year trends in stand density and stand basal area (Figure 11)

Figure 11

Simulated stand density (left panel) and stand basal area (right panel) over 50 years in flooded and non-flooded plots.

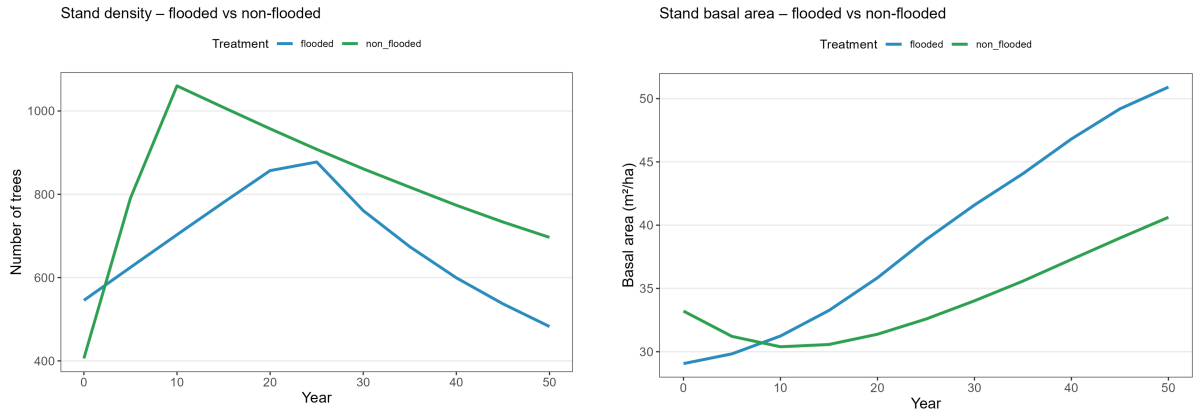

Note. Values represent stem density (number of trees per hectare). Blue line = Flooded ; Green line = Non-flooded .

In both treatments, stand density shows clear changes over time . In flooded plots, tree numbers start around 545 trees per hectare and increase to a peak of about 877 trees per hectare at year 25. After that, density declines steadily to roughly 483 trees per hectare by year 50. In non-flooded plots, density rises much more strongly at first, from about 400 to more than 1 060 trees per hectare at year 10, and then declines gradually to about 697 trees per hectare at year 50.

The stand basal area follows a different pattern. In flooded plots, basal area increases almost continuously from about 29 to 51 m² per hectare over the 50-year period. In non-flooded plots, basal area first decreases slightly during the first 10 years, then increases more slowly to about 41 m² per hectare by year 50. Overall, flooded plots end with higher basal area but lower stand density than non-flooded plots.

Table 5

Initial and 50-year stand attributes in flooded and non-flooded plots

Treatment	Year	Basal Area(m^2/ha)	Number of Trees ha^{-1}	Max DBH(cm)	D* index
Flooded	0	29.06	545.33	111	16
	50	50.91	482.51	127.53	31.5
Non-flooded	0	33.21	406	152	6
	50	40.62	696.54	164.02	21.96

The summary table (Table 5) confirms these patterns. Between year 0 and year 50, basal area increases more in flooded plots than in non-flooded plots, while stem density shows a smaller net change. Maximum DBH and canopy threshold (D*) also increase in both treatments, while largest dbh trees are in non flooded stands suggesting a higher share of very large trees there.Despite these differences, D* rose sharply in both scenarios, confirming that as the stands matured, it became increasingly difficult for smaller trees to retain a position in the upper canopy.

3.3 Biodiversity value and carbon storage

3.3.1 Tree Species Abundance

Figure 12

Tree Species Abundance

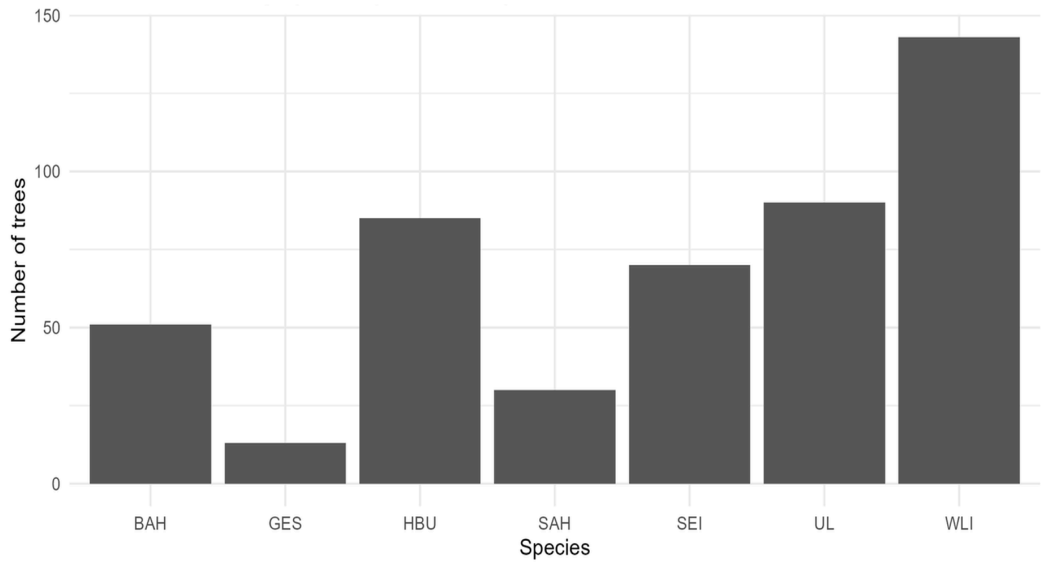

From the abundance data, it is evident that the forest is dominated by a small number of tree species, with Tilia(lime), Carpinus(hornbeam) and Quercus(oak) being the most abundant species in the forest inventory. These three tree genera have the highest number of recorded stems and basal area, while other tree genera have fewer individuals and contribute less to the abundance. This suggests that forest has an uneven and oligodominant abundance distribution pattern.

Such skewed abundance patterns are typical for temperate floodplain forests, where a small number of competitively successful, long-lived hardwood species form the structural core of the community and less abundant species occupy more specialised or transient niches (Turner et al., 2004; Naiman et al., 2005). From an ecological point of view, the dominance of lime, hornbeam and oak suggests that the structure of the canopy cover, the amount of resources available, and the number of microhabitats are largely determined by the presence of these species, whereas the rare species make a relatively minor contribution to the structure of the stand (Dobrowolska 2008; Ville Walder n.d.)

3.3.2 Mean DBH variation among tree species

Figure 13

Mean DBH among Tree species

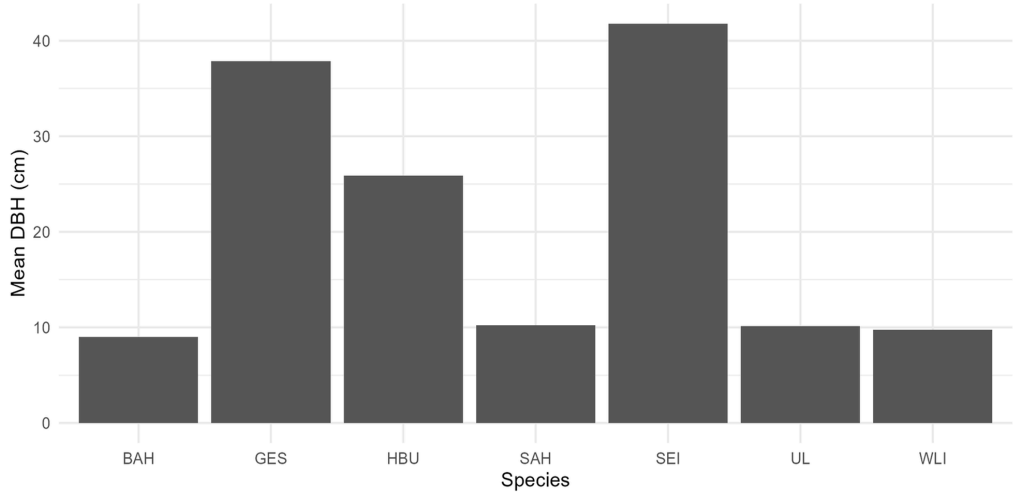

The mean diameter at breast height (DBH) also varies considerably among the different tree species in the study species in the study sites, where the Quercus (oak) and Fagus have the maximum mean DBH. This suggests the presence of mature, large statured individuals that

significantly affect the forest structure, especially through their contribution to canopy height, basal area, and mechanical stability. Large mean DBH values are evident for these species, reflecting their longevity and competitive ability in the floodplain environment, where they form the upper canopy layer, controlling light penetration to the lower strata.

From an ecological perspective, these large trees have a disproportionate effect on resource capture (light, water, nutrients) and critical microhabitats such as bark crevices and dead wood, whereas species with smaller mean DBH have a subordinate role in the understory (Collins et al., 2012; Turner et al., 2004). This size differentiation aligns with floodplain forest dynamics, where dominant canopy species maintain structural complexity over decades, supporting higher biodiversity than even-sized stands (Haase et al., 2009).

3.3.3 Mean growth rate across tree species

Figure 14

Mean Growth rate across tree species

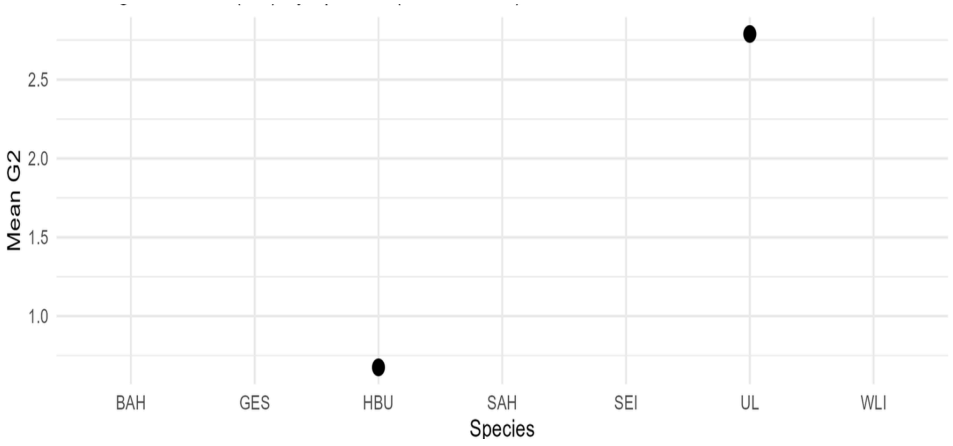

Mean annual growth rates vary considerably from one tree species to another, with some genera having high growth rates despite being less abundant or having less average size. From these results, it shows that individual growth performance does not relate to structural dominance at the stand level, where contribution of each species depends on the combined effect of growth rate, abundance and maximum potential size. Faster growing but less abundant species may thus contribute disproportionately little to canopy closure, basal area accumulation, or overall biomass compared to slower growing dominants like oak.

3.3.4 Carbon storage estimation

Figure 15

Carbon Storage estimation

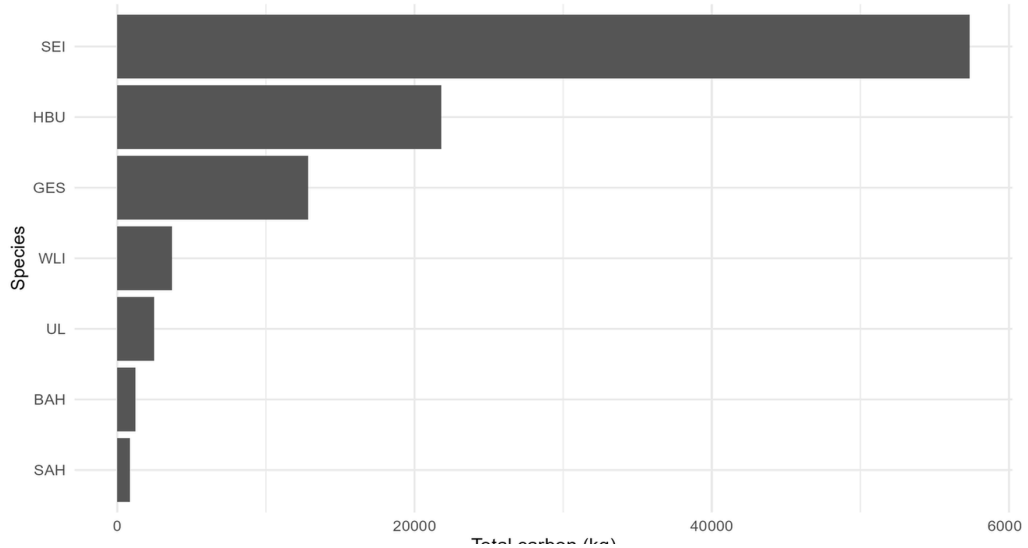

The above-ground stock in the plots is dominated by Quercus, with the amount of carbon stored by this genus far exceeding that stored by all other tree species combined. This is due to the combined effect of the relatively large mean DBH of Quercus and the density of the wood. The reason for this dominance of Quercus is that the estimates of carbon stock from allometric equations vary non-linearly with tree size. The oak-dominated carbon stocks also demonstrate the importance of the species as a long term carbon storage component in floodplain forests, where mature individuals survive multiple flood events and accumulate biomass over long periods.

Likewise, the biodiversity index at the forest level - obtained by weighting the diversity scores by the basal area occupied by each genus - shows Quercus by far the most important genus, with the highest contribution due to its high structural importance and very high relevance to saproxylic beetles. Other genera, such as Fraxinus (ash), Tilia(lime), Ulmus(elm), and Acer (maple), contribute much less to the index. The dominance of oak in controlling both carbon and biodiversity is consistent with its established position as a framework species in European floodplain forests, where large oak trees leave behind structural legacies that support dependent species even after their own death (Boyce et al., 2025; Henkel et al., 2025).

3.3.5 Forest Biodiversity value Index

To assess how forest structure translates into functional biodiversity outcomes, a forest biodiversity value index was calculated by integrating tree structural dominance with tree genus specific beetle diversity relevance indices

Figure 16

Biodiversity Value Index

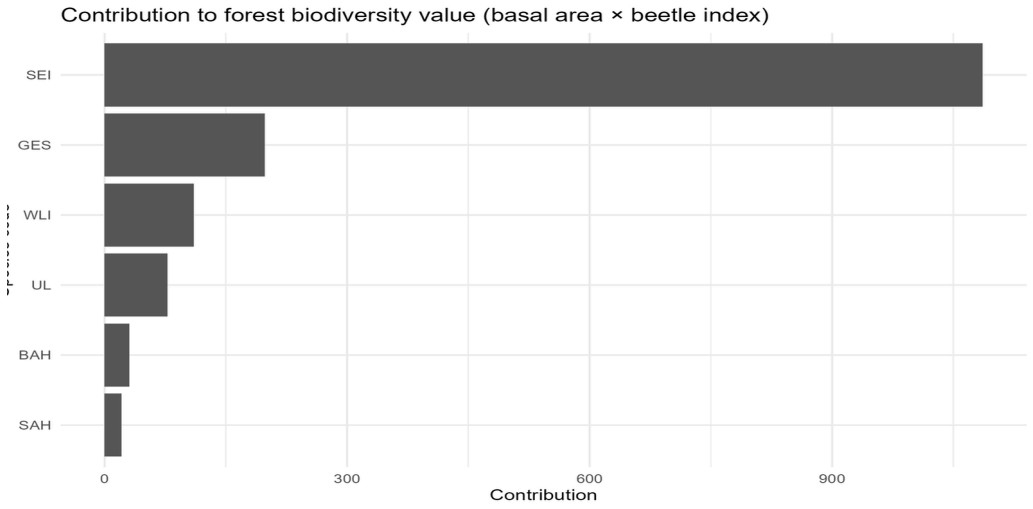

This figure demonstrates the contribution of various tree species to the forest biodiversity value index. Biodiversity value was found to be distributed in an uneven manner among the species groups. A few species contributed significantly to the value index. Quercus (oak) tree species had the highest contribution to the biodiversity value. The contribution of oak tree species was found to be significantly higher than the other tree species. The higher contribution of oak species to the biodiversity value was due to the combination of structural dominance of the tree species in terms of basal area and high values of beetle diversity relevance for tree species.

The contribution of other tree species such as Fraxinus, Tilia, Ulmus and Acer to the biodiversity index is significantly lower if compared to oak tree species. Some of the tree species in the other species group were found to be abundant in terms of stem count; contribution of the tree species group to the biodiversity value was lower due to the basal area or the lower beetle diversity relevance score. Overall the biodiversity value index was strongly shaped by differences in tree size structure and species dominance rather than by species abundance alone.

4. Discussion

4.1 Demographic Responses To Flooding

Demographic results of this study demonstrate that regular flooding is a central driver of floodplain forest structure and development in the Elster–Luppe system. Empirical inventory data from flooded plots show that shade- and flood-tolerant species such as lime (*Tilia cordata*), hornbeam (*Carpinus betulus*), elm (*Ulmus* spp.), and Norway maple maintain stable growth and successful regeneration under recurrent inundation, whereas ash (*Fraxinus excelsior*) and oak (*Quercus robur*) exhibit reduced growth and limited regeneration due to flood stress, shading, and disease effects. Tree mortality remains generally low across flooding regimes, indicating that flooding does not trigger abrupt forest decline but instead shapes forest dynamics gradually through demographic filtering. These patterns closely align with findings from the regional reference study by Elles (2025), which, based on a larger and longer-term dataset, similarly identified flooding as a selective ecological filter. Together, the results support controlled flooding as an effective management strategy to promote resilient, near-natural floodplain forests, while highlighting the need for targeted interventions if oak conservation is a specific management objective.

4.2 Species Composition And Size Structure

4.2.1 Shifts in Species Dominance and Hydrological Filtering

The simulation results in section 3.2.1 shows a clear split in which species dominate over the long term, driven by their differing ability to tolerate floods. Oak (*Quercus robur*) and Elm (*Ulmus minor*) expand their basal area because they are physiologically equipped to handle low-oxygen conditions in the soil. Specifically, these species can sustain growth during waterlogging by accelerating sugar breakdown (glycolysis) and forming porous stem structures (lenticels) to breathe. These adaptations effectively solve the cellular energy crisis that usually stops tree growth (Kreuzwieser & Rennenberg, 2014).In contrast, the Sycamore Maple (*Acer pseudoplatanus*) declines because it is highly sensitive to oxygen deprivation. Lacking the robust metabolic and physical adaptations of Oak and Elm, the Maple suffers from energy starvation and stops accumulating biomass (Glenz et al., 2006; Kreuzwieser & Rennenberg, 2014). However, the simulation also predicts a rise in Hornbeam (*Carpinus betulus*) and Lime (*Tilia*). Although they have only intermediate tolerance (30–35 days), they are still more resilient than the sensitive Maple(Kreuzwieser & Rennenberg, 2014). This slight physiological advantage

allows them to survive the stress and take over the space and resources left behind by the dying Maple population, a pattern best described as competitive release.

In the non-flooded scenario, Sycamore (*Acer pseudoplatanus*) and Norway Maples (*Acer platanoides*) establish dominance by leveraging their rapid growth rates. As gap specialists, these species form broad, dense canopies that intercept the majority of available light (Petriţan et al., 2009). This creates an environment of deep shade, which severely impacts the Oak (*Quercus robur*) population. Because Oak is a light-demanding species, its regeneration fails under this closed canopy, leading to a 50% decline in basal area as mature trees are not replaced. In contrast, Hornbeam (*Carpinus betulus*) and Lime (*Tilia*) exhibit a minimal increase in basal area. Their high shade tolerance allows them to persist in the understory where Oak seedlings perish (Hagemeier & Leuschner, 2019), yet their expansion is limited by the intense competitive pressure from the dominant maples

The sharp decline of *F. excelsior* across both scenarios reflects the elevated mortality rates parameterized in the model, consistent with regional observations of ash dieback (Henkel et al., 2025).This mortality creates canopy gaps that drive divergent successional outcomes.In flooded conditions, these openings facilitate the recruitment of a diverse, flood-tolerant community. In contrast, non-flooded gaps are rapidly monopolized by competitive maples, leading to a simplified and dense forest composition.

4.2.2 Contrasting Structural Dynamics: Self-Thinning vs. Competitive Stagnation

The structural development of the forest differs significantly between treatments (section 3.2.2). In the flooded scenario, the forest demonstrates a trajectory of maturation and efficient self-thinning. The initial cohort of small stems successfully recruited into larger size classes (20-60 cm), driving a continuous increase in stand basal area (51 m²/ha) while stem density declined to stable levels. This negative relationship between density and tree size is consistent with the self-thinning rule (Zeide, 1991), indicating that survivor trees are effectively converting resources into individual biomass expansion (Pretzsch, 2009).

However, the non-flooded scenario shows a trajectory of competitive stagnation. Rapid recruitment of shade-tolerant maples led to a density surge (>1,000 trees/ha), yet the Year 50 structure remains concentrated in smaller size classes (20-30 cm). This 'crowding effect' characterized by higher final density (696 trees/ha) but lower total basal area indicates that intense competition within species is limiting individual diameter growth (Zeide, 1991). Furthermore, the loss of basal area in the largest size classes confirms that the dense maple

canopy is preventing the recruitment of large canopy trees, a structural simplification typical of shade-tolerant dominance (Petriţan et al., 2009)

4.3 Biodiversity Value And Carbon Storage

4.3.1 Forest structure as a driver of biodiversity value

This study proves that the value of forest biodiversity is significantly affected by tree structural dominance rather than the number of species present. A few tree species were found to have a significant impact on the total biodiversity value index. Among these species, oak trees showed the maximum contribution to the biodiversity value index due to the large basal area and beetle diversity relevance.

The dominance of oak trees is also evident from the fact that many tree species have been found to possess exceptionally high values of insect diversity due to their longevity and the provision of habitat for beetles through the presence of coarse bark and dead wood (Southwood, 1961; Seibold et al., 2015). By combining the basal area with beetle diversity relevance, the biodiversity value index gives both habitat quantity and habitat quality. This says that the assessments which are solely based on tree species richness or stem counts may underestimate the functional importance of large habitat - providing tree species (Pretzsch, 2009).

4.3.2 Growth rate versus Structural importance

The growth rates showed species-specific differences, but these growth rates were not correlated with biodiversity value or carbon storage. So, it shows that species with high growth rates will not necessarily have high biodiversity value, but species with low growth rates, i.e. long lived species, dominate the biodiversity index. The decoupling between growth and ecological performance was also found in forest ecosystems, where long term structural characteristics of species rather than growth drive the provision of habitats and ecosystem (Purves et al., 2008).

4.3.3 Carbon storage and its relationship to Biodiversity value

The carbon storage is also unevenly distributed among tree species, with oak contributing the largest share of above ground carbon stocks. This pattern shows the non linear relationship between tree diameter and biomass, whereby large trees dominate carbon storage at stand level (Pan et al., 2011; Chave et al., 2014).

Although biodiversity value and carbon storage are two distinct functions of ecosystems, they are driven by the same factor, which is the large, structurally dominant trees in this forest. The driving mechanism for both functions are different, carbon storage is biomass, for biodiversity value it is habitat relevance. So, high carbon storage does not necessarily mean high biodiversity value, though they coincide in the case of oak trees.

4.3.4 Forests Biodiversity Value Index

The results from the forest biodiversity value index showed that biodiversity value is highly concentrated in a few structurally dominant tree species, and the dominant species was Quercus (oak) by far. This result shows that biodiversity value in the forest level is not equally distributed among species and measured but cannot be represented by tree species richness and stem abundance alone; the biodiversity value is represented by the combination of tree structural dominance and species specific habitat relevance.

By combining basal area and beetle diversity relevance, the biodiversity value index accounts for both habitat quantity and quality. The results show that tree species richness and stem number based assessments might not be sufficient to reflect the functional role of large habitat-providing tree species. In floodplain forests, the presence of structurally dominant tree species like oak is likely to be crucial for the maintenance of high biodiversity value under ongoing restoration and management processes (Pretzsch, 2009; Naiman et al., 2005)

4.4 Limitations

The study’s findings are influenced by the small spatial extent of the sample plots. This limits how well the results represent the wider floodplain’s stand structure and species composition. In addition, it was challenging to accurately estimate demographic rates for all species due to the very short census period (4–5 years). Particularly, insufficient data were present to calculate common ash (Fraxinus excelsior) growth rate and mortality rates for several other species, requiring the use of external estimates.Additionally, there are inherent shortcomings in the demographic models. The projections mostly reflect the internal assumptions of the PPA model, which was parameterized using this limited field data. Moreover, unpredictable occurrences like major disturbances, which have the potential to drastically change future forest dynamics, are not taken into consideration in the models.

5. Conclusion

The analysis of species-specific growth, mortality, and recruitment rates and simulation pattern shows that recurrent flooding strongly influences tree demography in the Elster–Luppe floodplain, favoring flood- and shade-tolerant species while constraining the performance and regeneration of flood-sensitive and light-demanding species due to their physiological adaptive capacity.

The simulation patterns also indicate that flooding favours species with high to moderate flood tolerance due to their physiological adaptive capacity. However, flooding also leads to reduced stem density caused by higher mortality rates. Moreover, the surviving trees contribute to increased basal area and a higher abundance of large trees, shifting species dominance. These findings suggest that flooding substantially modifies both tree species composition and size structure in floodplain forests.

This research shows that flooding is a significant factor in the formation of forest structure and, consequently, in biodiversity value and carbon storage in floodplain forests. The differences between flooded and non flooded areas were mainly expressed in the structural characteristics of the forest, such as species composition, size distribution, and basal area. These structural differences resulted in differences in biodiversity value and carbon storage depending on the hydrological regime. In general, the data shows that flooding has an indirect effect on biodiversity value and carbon storage by affecting forest structure, rather than species abundance. The results of this research emphasize the significance of the hydrological regime in the restoration and management of floodplain forests, as the restoration of natural flooding regimes can have a long term effect.

6. References

Bayley, P. B., & Sparks, R. E. (1989). The Flood Pulse Concept in River-Floodplain Systems.

Boyce, J., Elles, L., Henkel, S., Kasperidus, H. D., Padberg, A., Scholz, M., Schorn, M. E., Sickert, A., Vieweg, M., & Rüger, N. (2024b). How can oak regeneration in the Leipzig Floodplain Forest be effectively supported by femel plantations? Application of a demographic forest model. *Ecological Modelling*, *499*(110920). https://doi.org/10.1016/j.ecolmodel.2024.110920

Chave, J., Méchain, M. R., Alberto Búrquez,, Chidumayo, E., Colgan, M. S., & Delitti, W. C. (2014, October). Improved allometric models to estimate the aboveground biomass of tropical trees. *Global Change BiologyVolume 20, Issue 10 pp. 3177-3190Global Change BiologyVolume 20, Issue 10 pp. 3177-3190*. https://doi.org/10.1111/gcb.12629

Engelmann, R. A., Seele-Dilbat, C., Hartmann, T., Pruschitzki, U., Kasperidus, H. D., Scholz, M., & Wirth, C. (2022). Der Gehölzbestand des Stieleichen-Ulmen-Hartholzauenwalds im Projektgebiet Lebendige Luppe. In M. Scholz (Ed.), *Die Elster-Luppe-Aue – eine wertvolle Auenlandschaft* (pp. 115-132). Helmholtz-Zentrum für Umweltforschung (UFZ).

Glenz, C., Schlaepfer, R., Iorgulescu, I., & Kienast, F. (2006). Flooding tolerance of Central European tree and shrub species. *Forest Ecology and Management*, *235*(1-3), 1-13. https://doi.org/10.1016/j.foreco.2006.05.065

Hans Pretzsch. (2010, January). Forest dynamics, growth and yield. 10.1007/978-3-540-88307-4 1

Helmholtz Centre for Environmental Research (UFZ). (2024, May 22). *Natural climate protection: new water in historical rivercourses*. Retrieved January 21, 2026, from https://www.ufz.de/index.php?en=36336&webc_pm=17%2F2024

Henkel, S., Richter, R., Andraczek, K., & Mundry, R. (2024). Floodplain forests under stress: how ash dieback and hydrology affect tree growth patterns under climate change. (2024). 10.21203/rs.3.rs-4676274/v1

Henkel, S., Richter, R., Andraczek, K., Mundry, R., Dontschev, M. D., Engelmann, R. A., Hartmann, T., Hecht, C., Kasperidus, H. D., Rieland, G., Scholz, M., Seele-Dilbat, C., Vieweg, M., & Wirth, C. (2025). sh dieback and hydrology affect tree growth patterns under climate change in European floodplain forests. *Scientific Reports*, *15*(10117). https://doi.org/10.1038/s41598-025-92079-5

Hughes, F. M. R., & Rood, S. (2003, August). Allocation of River Flows for Restoration of Floodplain Forest Ecosystems: A Review of Approaches and Their Applicability in Europe. 10.1007/s00267-003-2834-8

Kreuzwieser, J., & Rennenberg, H. (2014). Molecular and physiological responses of trees to waterlogging stress. *Plant, Cell & Environment*, *37*(10), 2245-2259. https://doi.org/10.1111/pce.12310

Landesamt für Umweltschutz Sachsen-Anhalt. (2000). *LSG Elster-Luppe-Aue. In Die Landschaftsschutzgebiete Sachsen-Anhalts(Ergänzungsband 2003)*. LSG Elster-Luppe-Aue. Retrieved January 21, 2026, from https://lau.sachsen-anhalt.de/fachthemen/naturschutz/schutzgebiete-nach-landesrecht/landschaftsschutzgebiet-lsg/lsg45

Lebendige Luppe. (n.d.). *Lebendige Luppe – Revitalisierung der Elster-Luppe-Aue von Leipzig bis Schkeuditz*. Bundesamt für Naturschutz (BfN). Retrieved January 21, 2026, from https://www.bfn.de/projektsteckbriefe/lebendige-luppe

Mildrexler, D. J., Berner, L. T., Law, B. E., Richard A. Birdsey, & Moomaw, W. R. (2020). Large Trees Dominate Carbon Storage in Forests East of the Cascade Crest in the United States Pacific Northwest. 10.3389/ffgc.2020.594274

Oliver, C. D., & Larson, B. C. (1996). Brief Notice: Forest Stand Dynamics (Update Edition). *Forest Science*, *42*(3), 397. https://doi.org/10.1093/forestscience/42.3.397

Pan, Y., Birdsey, R. A., Fang, J., & Houghton,, R. (2011). A Large and Persistent Carbon Sink in the World's Forests. 10.1126/science.1201609

Pan, Y., Birdsey, R. A., Fang, J., & Houghton, R. A. (2011). A Large and Persistent Carbon Sink in the World's Forests. 10.1126/science.1201609

Petriţan, A.M., von Lu¨pke, B., & Petriţan, I. C. (2009). Influence of light availability on growth, leaf morphology and plant architecture of beech (Fagus sylvatica L.), maple (Acer pseudoplatanus L.) and ash (Fraxinus excelsior L.) saplings. *European Journal of Forest Research*, *128*, 61-74. 10.1007/s10342-008-0239-1

Pretzsch, H. (2009). *Forest Dynamics, Growth and Yield: From Measurement to Model*. Springer Berlin Heidelberg.

Purves, D. W., & Lichstein, J. W. (2007). Crown plasticity and competition for canopy space: a new spatially implicit model parameterized for 250 North American tree species. PloS one, 2(9), e870. (2007). https://doi.org/10.1371/journal.pone.0000870

Purves, D. W., Lichstein, J. W., & Pacala, S. W. (2007). Crown plasticity and competition for canopy space: a new spatially implicit model parameterized for 250 North American tree species. (2007). https://doi.org/10.1371/journal.pone.0000870

Riparia: Ecology, Conservation, and Management of Streamside Communities. (n.d.). 10.1641/0006-3568(2006)56[353:FL]2.0.CO;2

Roman, L. A., & Scatena, F. N. (2011). Street tree survival rates: Meta-analysis of previous studies and application to a field survey in Philadelphia, PA, USA. *Urban Forestry & Urban Greening*, *10*(4), 269-274. https://doi.org/10.1016/j.ufug.2011.05.008

Rozendaal, D. M. A., et al. (2020). Competition influences tree growth, but not mortality, across environmental gradients. Ecology, 101(7), e03052.

Seibold, S., Bässler, C., Brandl, R., & Gossner, M. M. (2015). Experimental studies of dead-wood biodiversity — A review identifying global gaps in knowledge. (2015). 10.1016/j.biocon.2015.06.006

Strigul, N., Pristinski, D., & Purves, D. (2008). SCALING FROM TREES TO FORESTS: TRACTABLE MACROSCOPIC EQUATIONS FOR FOREST DYNAMICS. (2008). https://doi.org/10.1890/08-0082.1

T. R. E. Southwood. (1961). The Number of Species of Insect Associated with Various Trees. https://doi.org/10.2307/2109

Tockner, K., Uehlinger, U., & Robinson, C. T. (2010). Rivers of Europe. Academic Press.

Ward, J. V., Tockner, K., Arscott, D. B., & Claret, C. (2002). Riverine landscape diversity. Freshwater Biology, 47(4), 517–539.

Zeide, B. (1991, June). Self-Thinning and Stand Density. *Journal of Forestry*, *37*(2), 517–523,. https://doi.org/10.1093/forestscience/37.2.51.

Appendix A: Supplementary Materials

Figure A.1. Analysis of annual diameter growth rates (cm year^{-1}) versus initial DBH (cm) for identifying outliers. Points represent individual trees measured in 2020 and 2024/2025. Red dashed lines indicate the biological plausibility thresholds used for data cleaning (-1 to +1 cm year^{-1}). Observations outside this range (grey points) were excluded from the growth rate calculation to prevent artifacts from measurement errors. Panels show outliers removed from analysis for WLI in canopy 2 of flooded plot.

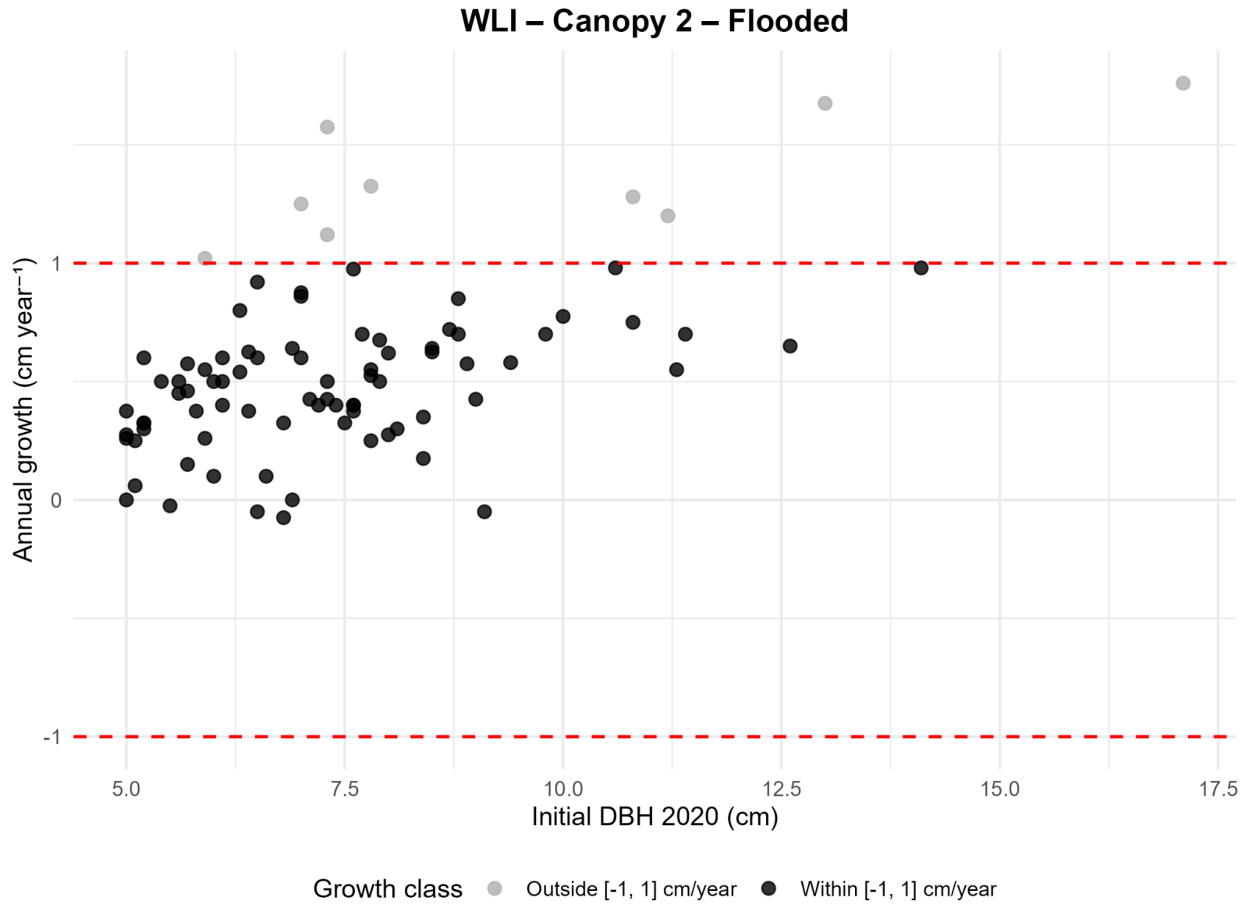

Table A.1. Lucian Elles data used in comparison to the field data inventory collected for 3 flooded and 2 non-flooded plots. This data covered a total of 60 permanent plots and comprised 8491 individual trees.

species	G1 (cm/yr)	G2 cm/yr)	mu1 (/yr)	mu2 (/yr)	Rec_ha (N/ha yr)
BAH	0.39	0.34	0.0368	0.0341	2.75
GES	0.25	0.14	0.0361	0.0748	0.35
HBU	0.33	0.28	0.0066	0.0066	0.82
SAH	0.42	0.33	0.008	0.0066	1.14
SEI	0.34	0.21	0.0195	0.0682	0
UL	0.33	0.26	0.0444	0.033	4.13
WLI	0.21	0.19	0.0117	0.0073	2.82

Table A.2. Final parameterization used for the PPA model simulations in the flooded plots. Growth rates for *Fraxinus excelsior* , zero-mortality values and crown allometry data were substituted with values from Boyce et al. (2025).

species	G1 (cm/yr)	G2 cm/yr)	mu1 (/yr)	mu2 (/yr)	Rec_ha (N/ha yr)	inflection	steepness	param1	param2
BAH	0.2114	0.1693	0.0382	0.0332	0.6667	65.58	22.3	-0.4	200
GES	0.1981	0.14	0.0653	0.0748	0.2667	77.06	18.06	10.31	250
HBU	0.3286	0.3422	0.0066	0.0066	2.6667	46.54	26.56	-29.13	200
SAH	0.4658	0.3688	0.008	0.0066	3	65.58	22.3	-0.4	200
SEI	0.3306	0.1643	0.006	0.0271	0	77.06	18.06	10.31	250
UL	0.5179	0.4673	0.0682	0.0199	5.4667	64.93	19	-0.5	200
WLI	0.523	0.4679	0.0117	0.002	10.6	64.93	19	-0.5	200

Table A.3. Final parameterization used for the PPA model simulations in the non-flooded plots. Growth rates for *Fraxinus excelsior* , zero-mortality values and crown allometry data were substituted with values from Boyce et al. (2025).

Species	G1 (cm/yr)	G2 cm/yr)	mu1 (/yr)	mu2 (/yr)	Rec_ha (N/ha yr)	inflection	steepness	param1	param2
BAH	0.4364	0.5473	0.0312	0.0341	72.5	65.58	22.3	-0.4	200
GES	0.0559	0.14	0.0515	0.0748	0	77.06	18.06	10.31	250
HBU	0.375	0.3833	0.0066	0.0066	0.5	46.54	26.56	-29.13	200
SAH	0.5938	0.5114	0.008	0.0066	11	65.58	22.3	-0.4	200
SEI	0.2404	0.3	0.0195	0.0682	0	77.06	18.06	10.31	250
UL	0.3375	0.3422	0.029	0.033	1.5	64.93	19	-0.5	200
WLI	0.4679	0.4739	0.0117	0.0073	2	64.93	19	-0.5	200